Annals of Nuclear Medicine Vol. 20, No. 4, 295–301, 2006

# Comparisons of the time-activity curves of the cardiac blood pool and liver uptake by $^{99m}$Tc-GSA dynamic SPECT and measured $^{99m}$Tc-GSA blood concentrations

Yukio SUGAI, Akio KOMATANI, Takaaki HOSOYA and Kazue TAKAHASHI

*Department of Radiology, Yamagata University School of Medicine*

***Objectives:*** The aim of this study was to determine the time-activity curve in the cardiac and hepatic region by $^{99m}$Tc-GSA dynamic SPECT which is clinically used in liver scintigraphy and evaluate the temporal changes in the consistency and errors at the absolute scale using the regression equation of changes in the blood concentration of $^{99m}$Tc-GSA. ***Methods:*** In 11 patients who underwent $^{99m}$Tc-GSA dynamic SPECT over the 30 min period after IV injection, the percentages of activity in the collected blood and in the blood pool estimated by dynamic SPECT were determined as the plasma clearance by blood collection and as the blood clearance by cardiac pooling. Extrahepatic uptake, expressesd as 100 – (% uptake in the liver by dynamic SPECT (%)) was calculated as the blood clearance by the liver. The regression equation ($Y = Y_0 + Ae^{-\alpha t}$) was determined from the changes in the counts, expressed as a percent. Percent errors and the differences in the $Y$-intercept ($Y_0$), coefficient ($A$) and slope ($\alpha$) on the regression curve were compared. ***Results:*** Blood pool clearance gradually exceeded the measured plasma clearance. The clearance by the liver started from a very low initial value and gradually became equal to that of plasma clearance over the first 15 minutes and exceeded it over the second 15 minutes. The $Y$-intercept was significantly higher in the blood pool clearance than that in the measured plasma clearance ($p < 0.001$), and the coefficient was significantly lower in the former than the latter ($p < 0.001$). The coefficient and slope were significantly lower in the hepatic clearance than the plasma clearance ($p < 0.001$, $p < 0.005$). ***Conclusion:*** The time-activity curve of the blood pool showed a tendency towards overestimation in the second half of the examination, probably due to scatter effect from the liver. The time-activity curve of liver uptake showed a tendency towards overestimation in the first half of the examination, probably due to the high concentration in the hepatic blood pool, and underestimation in the second half.

**Key words:** $^{99m}$Tc-GSA, SPECT, liver, blood-pool scintigraphy

## INTRODUCTION

$^{99m}$Tc-DTPA-galactosyl human serum albumin ($^{99m}$Tc-GSA) is a radiopharmaceutical that binds specifically to asialo-glyco-protein receptors on the liver cell membrane.[1–3] Since receptor numbers are decreased in hepatopathy, accumulation of $^{99m}$Tc-GSA in the liver measured by scintigraphy correlates well with liver function tests.[4–7] Liver scintigraphy using $^{99m}$Tc-GSA is widely used for evaluation of hepatic function and functional reserve, and various methods for the quantitative analysis of time-activity curves have been reported.[8–12] However, there are differences between the time-activity curves for the blood pool and liver and actual measured concentrations of $^{99m}$Tc-GSA in blood and hepatic parenchyma. There have been no studies examining their consistency, or the changes in errors with time at the absolute scale. The reliability of the time-activity curve used to determine blood pool concentration remains unclear. We determined the time-activity curves in the blood pool and hepatic regions by continuous dynamic $^{99m}$Tc-GSA SPECT over the 30 minutes following injection, and evaluated the

Received August 29, 2005, revision accepted March 13, 2006.

For reprint contact: Yukio Sugai, M.D., Department of Radiology, Yamagata University School of Medicine, Iida-Nishi 2–2–2, Yamagata 990–9585, JAPAN.

E-mail: ysugai@med.id.yamagata-u.ac.jp

temporal changes in the consistency and errors using the absolute regression equation for changes in the blood concentration of $^{99m}$Tc-GSA and its measurements obtained by simultaneous collection of serial blood samples.

## SUBJECTS

The subjects consisted of 11 patients (5 males, 6 females, mean age 62 years, range 36–90 years) who underwent $^{99m}$Tc-GSA dynamic SPECT. Four had chronic hepatitis, 5 had cirrhosis, and 2 had hepatic tumor. Written informed consent was obtained from all patients.

## METHODS

*1. Dynamic SPECT protocol*

The dose of $^{99m}$Tc-GSA was 185 MBq (Nihon Medi-Physics, Nishinomiya, Japan). We used a three-headed gamma camera (MULTISPECT 3, Siemens Medical Systems, Erlangen, Germany) with the following parameters: imaging for 2 min (120 degrees/head for 24 views) was performed 5 times between 2 and 12.5 minutes after injection, followed by imaging for 2.5 minutes (120 degrees/head for 24 views) back and forth (5 minutes) performed 4 times between 12.5 and 33.5 minutes after injection. The total imaging time was 30 min (9 segments), consisting of 2-min imaging × 5 and 5-min imaging × 4 segments. Dynamic SPECT of the syringe before injection was performed for 12 seconds (120 degrees/head, 24 views) to measure the total injected dose. All imaging was done with a 64 × 64 matrix.

*2. Time-activity curves*

Images were reconstructed by the filter convolution method, and the attenuation was corrected by Chang's method. Data were not corrected for scatter. The cut-off at the periphery was 0% for the syringe and 34% for the liver. The latter value for functional liver volume was experimentally chosen to agree with the liver volume measured by CT in our hospital. SPECT images of the blood pool were calculated by raw projection data, and 10–15 images of the heart and large blood vessels distant from the liver were chosen. The ROI including the heart and descending aorta was defined, and a time-activity curve generated (Fig. 1). The ROI for the liver was similarly defined on SPECT images.

*3. Measurement of the blood concentration of $^{99m}$Tc-GSA*

The radioactivity value of $^{99m}$Tc-GSA dosage (the syringe before injection) was measured by the dilution method using a well scintillation counter before imaging. After IV administration of the $^{99m}$Tc-GSA into an antecubital vein, blood samples were collected from the contralateral vein. Blood was collected 7 times, at 3, 5, 7, 10, 15, 20, and 30 minutes after injection, and the concentration of $^{99m}$Tc-GSA measured with a scintillation counter.

*4. Standardization of the time-activity curve and the regression equation*

Percentages of the activity in the collected blood and in the blood pool estimated by dynamic SPECT against the dose were determined as the plasma clearance calculated from blood samples and as the estimated clearance by the blood pool. Similarly, the percentage of the activity in the liver by dynamic SPECT was determined, and the non-uptake in the liver (100 – uptake in the liver (%)) was calculated as the blood clearance by the liver for easier comparisons.

The regression equation, which was expressed as an $Y$-intercept + a monoexponential function ($Y = Y_0 + Ae^{-\alpha t}$), was determined from the changes in the count level (%) in each patient using the nonlinear least squares method.[13] Instead of general standard blood method, the regression equation was normalized with $Y$, namely, the dose of GSA at $t = 0$ as 100. Figure 2 shows the evaluation using the regression equation. In the early stage after administration (0–30 min), the $Y$-intercept ($Y_0$) shows the amount of $^{99m}$Tc-GSA remaining in the blood, the coefficient ($A$) shows the amount of $^{99m}$Tc-GSA taken up by the liver (binding to receptors), and the slope ($\alpha$) shows the rate of accumulation of $^{99m}$Tc-GSA in the liver and its clearance from the blood.[13]

*5. Evaluation of the time-activity curve*

Percentage errors of the clearance calculated with dynamic SPECT against the clearance derived from blood sample measurements and the hepatic clearance against the measured plasma clearance were determined from the regression curve 3, 5, 7, 10, 15, 20, 25, and 30 min after administration.

Differences in the $Y$-intercept ($Y_0$), coefficient ($A$), and slope ($\alpha$) on the regression curve were examined between the plasma and blood pool values and between the plasma clearance and hepatic clearance.

## RESULTS

Figure 3 shows the temporal changes in the percent error of the blood pool clearance compared with the plasma clearance. In the early phase, both levels were highly consistent; however, the clearance rate calculated by SPECT exceeded the measured clearance progressively with time, indicating a tendency to overestimation.

Figure 4 shows the temporal changes in the percent error of the hepatic clearance against the plasma clearance. Immediately after administration, the rate of hepatic clearance was very low, representing underestimation, and gradually increased until it was equal to the plasma clearance at about 10 min after administration and greater than plasma clearance after that, showing a tendency to overestimation.

Figure 5 shows a comparison between the regression equations for the plasma clearance and the blood pool

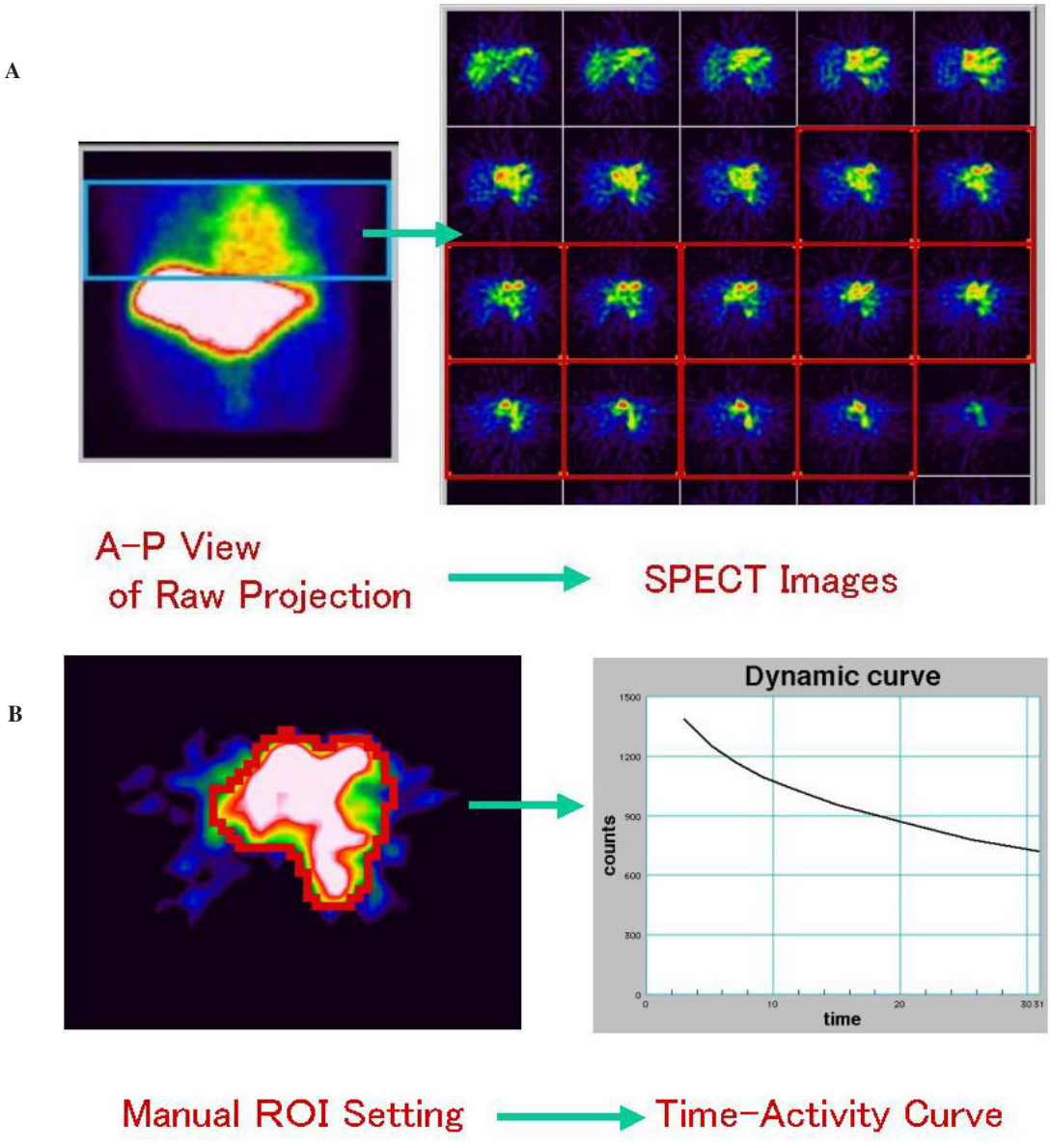


**Fig. 1** Generation of the time-activity curve of the blood pool. A: SPECT images of the cardiac region were calculated by raw projection of data, and 10–15 images of the heart and large blood vessels distant from the liver were chosen (*red frames*). B: A ROI including the heart and the descending aorta was drawn (*red line*), and a time-activity curve generated.

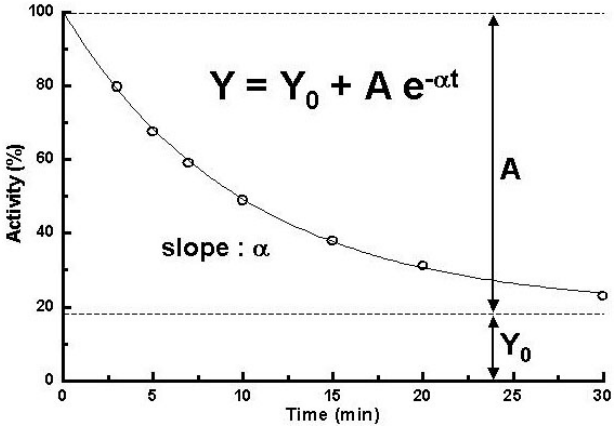


**Fig. 2** Evaluation by regression equation. We hypothesized that the blood kinetics of GSA could be described by a one-compartment model expressed as a monoexponential function with a *Y*-intercept ($Y = Y_0 + Ae^{-\alpha t}$). The *Y*-intercept ($Y_0$) shows the amount of $^{99m}$Tc-GSA remaining in the blood, the coefficient ($A$) shows the amount of $^{99m}$Tc-GSA taken up in the liver (binding to receptors), and the slope ($\alpha$) shows the rates of accumulation of $^{99m}$Tc-GSA in the liver and its clearance from blood.

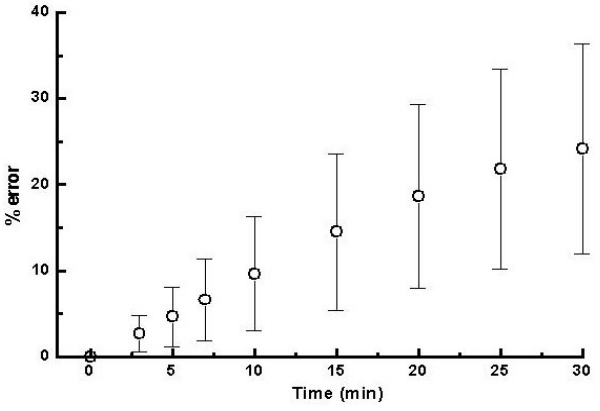


**Fig. 3** Changes in the % error of the clearance by blood pool against the measured plasma clearance. In the early phase both clearance rates were highly consistent. The blood pool clearance then gradually exceeded the plasma clearance.

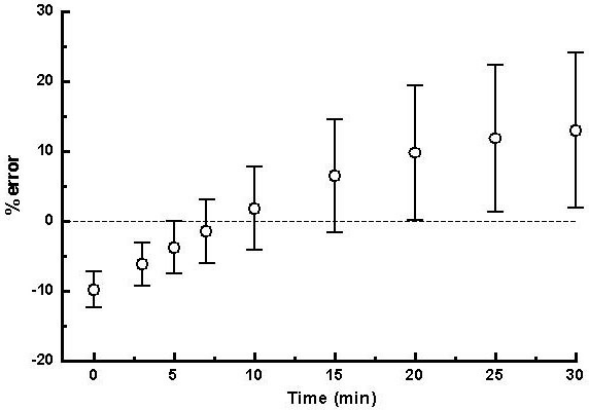


**Fig. 4** Changes in the % error of the hepatic clearance against the plasma clearance. Immediately after administration, the rate of hepatic clearance was very low and gradually increased, becoming similar to the rate of plasma clearance at about 10 min and then progressively exceeding the plasma clearance.

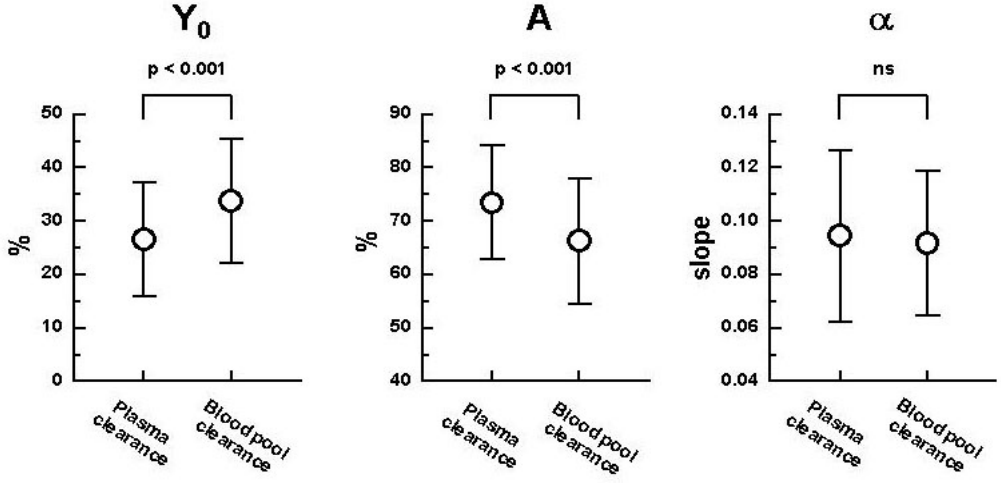


**Fig. 5** Comparison of the regression equations of plasma clearance and blood pool clearance. The *Y*-intercept was significantly higher for the blood pool clearance than for the measured plasma clearance ($p < 0.001$), and the coefficient was significantly lower in the former than the latter ($p < 0.001$).

clearance. The *Y*-intercept was significantly higher in the blood pool clearance than in the plasma clearance ($p < 0.001$), and the coefficient was significantly lower in the former than the latter ($p < 0.001$). No significant difference in the slopes was observed.

Figure 6 shows a comparison of the regression equations for the plasma clearance and the hepatic clearance. No significant difference was observed in the *Y*-intercepts of the two clearances. The coefficient and slope were significantly lower for the hepatic clearance as compared with the plasma clearance ($p < 0.001$, $p < 0.005$, respectively).

Figure 7 shows the regression curves of the plasma clearance and the blood pool clearance (7A) and the plasma clearance and hepatic clearance (7B) in a 58-year-old male patient with chronic hepatitis. The blood pool and plasma clearance rates started out equal, but the blood pool values gradually exceeded those of the plasma. The hepatic clearance started out lower than, and then gradually exceeded, the plasma clearance.

## DISCUSSION

There are various methods for the quantitative analysis of time-radioactivity curves by $^{99m}$Tc-GSA liver scintigraphy, ranging from simple methods such as the accumulation rate in the liver and the clearance rate from the blood[8,9] to compartment model analysis.[4,5,10–12] These methods are based on the hypotheses that all $^{99m}$Tc-GSA in the blood is taken up by the liver alone and that the small

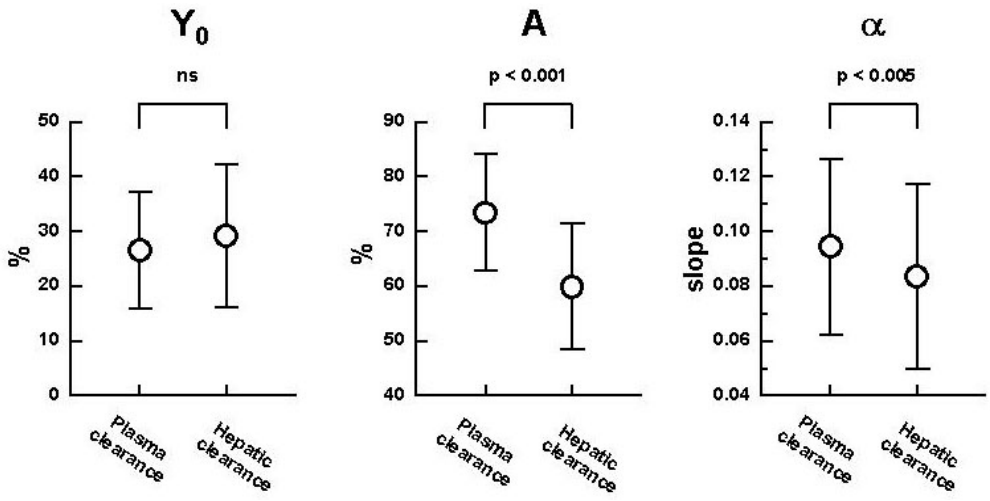


**Fig. 6** Comparison in the regression equations between the plasma clearance and the hepatic clearance. The coefficient and slope were significantly lower in the hepatic clearance than in the measured plasma clearance ($p < 0.001$, $p < 0.005$, respectively).

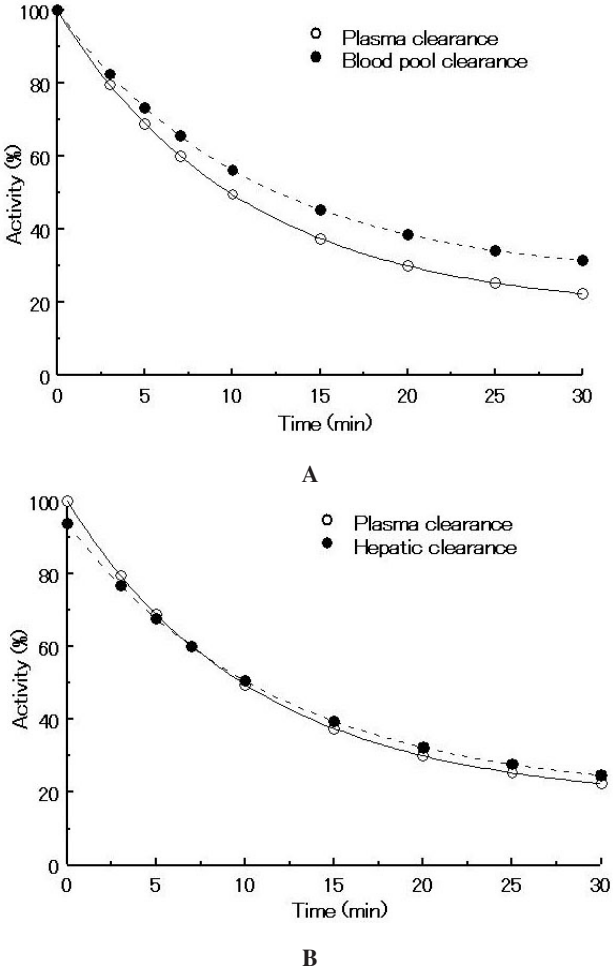


**Fig. 7** Representative regression curves of the clearance (58-y-old male with chronic hepatitis). A: Blood pool clearance vs. measured plasma clearance. The rate of blood pool clearance was gradually overestimated. B: Hepatic clearance vs. measured plasma clearance. The rate of hepatic clearance was underestimated immediately after administration.

amount of $^{99m}$Tc-GSA shifted to the interstitial fluid and excreted by the kidney is not yet clarified and is negligible.[12,14] Basically, the time-activity curve obtained by using ROIs in the liver and heart (blood pool) on planar or SPECT images is used as the parameter of accumulation in the liver and clearance from the blood. However, differences would exist between the time-radioactivity curve and the actual uptake in the liver or the blood concentration due to intrahepatic blood pooling, inter-operator variation, scatter, and statistical changes, etc. Only a few studies have shown that the time-activity curve correlates to some extent with the measured blood concentration from serial samples.[12,15] Except for only one report about validation of curve-fitting method with blood-sampling method,[16] no studies have examined the consistency of $^{99m}$Tc-GSA uptake or the changes in errors with time at the absolute scale. The reliability of the time-activity curve as an estimate of the blood concentration of $^{99m}$Tc-GSA remains unclear. This reliability has only been evaluated with a small number of blood collection points for comparison and with counts that are difficult to normalize. We have developed new software that enables us to generate time-activity curves in the liver and blood pool with continuous dynamic SPECT up to 30 minutes after administration. We performed absolute comparisons of time-activity curves rather than relative comparisons of measurement points under the same conditions by measuring the total dose and expressing it as a percentage, together with simultaneous blood sampling. The regression curve is based on our hypothesis. This hypothesis, of a non-linear, one-compartment model with an *Y*-intercept in the early phase after injection is supported by the blood levels of $^{99m}$Tc-GSA described in our previous report, where we demonstrated the consistency and usefulness of analysis in the early stage after injection (30 minutes).[13]

The clearance from the blood pool estimated by SPECT exceeded that from blood sample measurements in the second half of the examination. This was probably due to the strong effects of scattered ray on the cardiac region, where the $^{99m}$Tc-GSA concentration decreased as it was avidly taken up by the liver in the second half of the examination. This would have made the concentration of $^{99m}$Tc-GSA in the blood pool appear higher. However, the blood pool clearance agreed relatively well with the plasma clearance immediately after administration. Since changes in the count level in the blood are particularly large soon after administration and also large within one phase of the dynamic study, the concern arose that these large changes would result in inconsistencies. Taking this into consideration, the time for one phase of the dynamic SPECT program in our hospital was shortened in the first half of the 30-minute examination. The results obtained in the present study were considered to be better effected by averaging the radioactivity level due to the use of 3 detectors than by the shortened time of one phase. To use a simple method of producing the clearance curve by cardiac pooling obtained by dynamic SPECT as a substitution for the highly invasive and complicated plasma clearance, the differences in the late stage after administration must be solved. To eliminate the scattered ray from the liver, we have developed new software based on the dual energy window subtraction (DEWS) method proposed by Jaszczak et al.,[17] and are using it for scatter correction. Recently, SPECT equipment with included scatter correction software has been marketed, and is used in some facilities.[18]

The underestimation of the clearance of activity by liver in the first half of the examination was large, indicating that liver uptake was overestimated. Probably because of the very high blood concentration of $^{99m}$Tc-GSA and the low level of uptake in the liver in the first half of the examination, the contribution of counts from the hepatic blood pool and portal blood flow would have falsely elevated the estimation of hepatocellular uptake. Underestimation due to a cut-off level of 34% for imaging of the periphery, one of our concerns, was observed in the second half of the examination at the reduced blood concentration of $^{99m}$Tc-GSA due to decreased counts in the hepatic blood pool. But, underestimation in the second half cannot be explained only by these factors. Though attenuation correction and ROI selection may also influence these values, they remain an estimate. A large difference was observed in the clearance between hepatic uptake and plasma levels. Elimination of the error due to hepatic blood pool is difficult. However, since both clearance levels were relatively similar during the middle period of 10–15 min after administration, this period can be used to evaluate the liver uptake ratio and the blood clearance rate rather than the entire clearance curve of the liver. Before the introduction of dynamic SPECT into our hospital, we determined the liver uptake ratio 15 min after the administration of $^{99m}$Tc-GSA with SPECT (LUR15),[19] and are currently using the liver uptake ratio obtained by dynamic SPECT. The advantages of this method are that it involves few manual tasks such as ROI generation because it is mainly automated and has good reproducibility. SPECT effectively evaluates the volume and density of the liver. Additionally, using dynamic SPECT, delineation of change on standing and examination of the accumulation rate, gradient, etc., becomes possible.

## CONCLUSION

The blood pool time-activity curve using $^{99m}$Tc-GSA dynamic SPECT agreed well with the blood concentration measurements from samples drawn in the first half of the examination. However, in the second half, a tendency to overestimation was noted, probably due to the effects of scatter from the liver. The time-activity curve of liver uptake on dynamic SPECT showed a tendency to overestimation in the first half of the examination, probably due to the high concentration in the hepatic blood pool. In the second half, a tendency to underestimation was observed.

## REFERENCES


1. Morell AG, Gregoriadis G, Scheinberg IH, Hickman J, Ashwell G. The role of sialic acid in determining the survival of glycoproteins in the circulation. *J Biol Chem* 1971; 246: 1461–1467.
2. Ashwell G, Morell AG. The role of surface carbohydrates in the rat hepatic recognition and transport of circulating glycoprotein. *Adv Enzymol* 1974; 41: 99–128.
3. Stowell CP, Lee YC. Neoglycoproteins. The preparation and application of synthetic glycoproteins. *Adv in carbohydr Chem Biochem* 1980; 37: 225–281.
4. Stadalnik RC, Vera DR, Woodle ES, Trudeau WL, Porter BA, Ward RE et al. Technetium-99m NGA functional hepatic imaging: preliminary clinical experience. *J Nucl Med* 1985; 26: 1233–1242.
5. Galli G, Maini CL, Orlando P, Cobelli C, Thomaset K, Deleide G, et al. A radiopharmaceutical for the study of the liver: $^{99m}$Tc-DTPA-asialo-orosomucoid II: Human dynamic and imaging studies. *J Nucl Med Allied Sci* 1988; 32: 117–126.
6. Kubota Y, Kitagawa S, Inoue K, Ha-Kawa SK, Kojima M, Tanaka Y. Hepatic functional scintigraphic imaging with $^{99m}$Technetium galactosyl serum albumin. *Hepatogastroenterol* 1993; 40: 32–36.
7. Kudo M, Vera DR, Stadalnik RC, Trudeau WL, Ikekubo K, Todo A. *In vivo* estimates of hepatic binding protein concentration: Correlation with classical indicators of hepatic function reserve. *Am J Gastroenterol* 1990; 85: 1142–1148.
8. Kudo M, Todo A, Ikekubo K, Hino M, Yonekura Y, Yamamoto K, et al. Functional hepatic imaging with receptor-binding radiopharmaceutical: clinical potential as a measure of functioning hepatocyte mass. *Gastroenterol Jpn* 1991; 26: 734–741.
9. Koizumi K, Uchiyama G, Arai T, Ainoda T, Yoda Y. A new liver functional study using Tc-99m DTPA-galactosyl

human serum albumin: Evaluation of the viability of several functional parameters. *Ann Nucl Med* 1992; 6: 83–87.
10. Bossuyt A, De Geeter F, Jacobs A, Camus M, Thornback JR. Initial clinical experience with a new kit formulation of Tc-99m-galactosylated albumin for functional hepatic imaging. *Nucl Med Commun* 1990; 11: 469–475.
11. Vera DR, Stadalnik RC, Trudeau WL, Scheibe PO, Krohn KA. Measurement of receptor concentration and forward-binding rate constant via radiopharmacokinetic modeling of technetium-99m-galactosyl-neoglycoalbumin. *J Nucl Med* 1991; 32: 1169–1176.
12. Ha-Kawa SK, Tanaka Y. A quantitative model of technetium-99m DTPA-galactosyl-HSA for the assessment of hepatic blood flow and hepatic binding receptor. *J Nucl Med* 1991; 32: 2233–2240.
13. Sugai Y, Komatani A, Hosoya T, Takahashi K. Analysis of the early blood kinetics of $^{99m}$Tc-GSA and its verification: new one-compartment model and regression equation. *Nucl Med Commun* 2001; 22: 773–778.
14. Torizuka K, Ha-Kawa SK, Ikekubo K, Suga Y, Tanaka Y, Hino M, et al. Phase I Clinical Study on $^{99m}$Tc-GSA, a New Agent for Functional Imaging of the Liver. *KAKU IGAKU (Jpn J Nucl Med)* 1991; 28: 1321–1331.
15. Hwang EH. $^{99m}$Tc-GSA Dynamic SPECT for Regional Hepatic Functional Reserve Estimation: Assessment of Quantification. *KAKU IGAKU (Jpn J Nucl Med)* 1999; 36: 315–322.
16. Ha-Kawa SK, Suga Y, Kouda K, Ikeda K, Tanaka Y. Validation of curve-fitting method for blood retension of $^{99m}$Tc-GSA: Comparison with blood sampling method. *Ann Nucl Med* 1997; 11: 15–20.
17. Jaszczak RJ, Greer KL, Floid CE, Harris CC, Coleman RE. Improved SPECT quantitation using compensation for scattered photons. *J Nucl Med* 1984; 25: 893–900.
18. Ichihara T, Maeda H, Yamakado K, Motomura N, Matsumura K, Takeda K, et al. Quantitative analysis of scatter- and attenuation-compensated dynamic single-photon emission tomography for functional hepatic imaging with a receptor-binding radiopharmaceutical. *Eur J Nucl Med* 1996; 24: 59–67.
19. Sugai Y, Komatani A, Hosoya T, Yamaguchi K. Response to Percutaneous Transhepatic Portal Embolization: Evaluation of New Proposed Parameters by $^{99m}$Tc-GSA SPECT in Prognostic Estimation following Hepatectomy. *J Nucl Med* 2000; 41: 421–425.